$$\frac{\partial^2\xi}{\partial t^2}\pm\frac{\partial^2\xi}{\partial x^2}+\frac{1}{4}\frac{\partial^4\xi}{\partial x^4}+\frac{3}{4}\frac{\partial}{\partial x}\left(\frac{\partial\xi}{\partial x}\right)^2=0. \quad (35)$$

The upper sign of ξ_{xx} corresponds here to the above-threshold regime, and the lower one to the sub-threshold regime. We can write Eq. (35) in Hamiltonian form:

$$\partial\xi/\partial t=\delta H/\delta\eta, \quad \partial\eta/\partial t=-\delta H/\delta\xi, \quad (36)$$

where

$$H=\tfrac{1}{2}\int dx(\eta^2\mp\xi_x^2-\tfrac{1}{2}\xi_x^3+\tfrac{1}{4}\xi_{xx}^2). \quad (37)$$

The displacement ξ and velocity $\eta=\xi_t$ of the ions are here the canonically conjugate variables. As the Hamiltonian H does not depend explicitly on the time, Eq. (35) has an energy integral: $H=E=\text{const}$.

One can, using Eqs. (36), easily verify that the following relation holds:

$$\frac{d^2}{dt^2}\int dx\,\xi^2=-6E+\int dx\left(5\xi_t^2\mp\xi_x^2+\frac{1}{4}\xi_{xx}^2\right). \quad (38)$$

From this it clear that in the sub-threshold regime, when the second term on the right-hand side of (38) is positive, any perturbation with a negative energy grows without limit with time. The negative contribution to the energy is connected with the cubic terms in the Hamiltonian (37). Therefore, the corresponding perturbation must necessarily have an amplitude u of order unity. In terms of dimensional variables this critical amplitude is the smaller the closer the system is to the instability boundary.

[1)]From the degeneracy of the dispersion law for electromagnetic waves it follows that, strictly speaking, these waves are not characterized by the vectors S_2 and S_3, but by a polarization tensor. In introducing here the vectors S_2 and S_3 we imply, in fact, that there is some small perturbation which lifts the degeneracy.

[1]A. A. Vedenov and L. I. Rudakov, Dokl. Akad. Nauk SSSR **159**, 767 (1964) [Sov. Phys. Dokl. **9**, 1073 (1965)].
[2]A. A. Vedenov, A. V. Gordeev, and L. I. Rudakov, Plasma Phys. **9**, 719 (1967).
[3]A. A. Galeev, R. Z. Sagdeev, V. D. Shapiro, and V. I. Shevchenko, Zh. Eksp. Teor. Fiz. **73**, 1352 (1977) [Sov. Phys. JETP **46**, 711 (1977)].
[4]A. V. Gaponov and M. A. Miller, Zh. Eksp. Teor. Fiz. **34**, 242 (1958) [Sov. Phys. JETP **7**, 168 (1958)].
[5]V. E. Zakharov, Zh. Eksp. Teor. Fiz. **62**, 1745 (1972) [Sov. Phys. JETP **35**, 908 (1972)].
[6]E. A. Kuznetsov, Zh. Eksp. Teor. Fiz. **66**, 2037 (1974) [Sov. Phys. JETP **39**, 1003 (1974)].
[7]V. V. Krasnosel'skikh and V. I. Sotnikov, Fiz. Plazmy **3**, 872 (1977) [Sov. J. Plasma Phys. **3**, 491 (1977)].
[8]V. N. Tsytovich, Nelineĭnye éffekty v plazme (Non-linear effects in plasmas) Nauka, 1967 [English translation published by Plenum Press, New York].
[9]R. Pozzoli and D. D. Ryutov, Phys. Fluids **22**, 1782 (1979).
[10]V. E. Zakharov and A. B. Shabat, Funkts. Analiz **8**, 54 (1974) [Funct. Anal. Appl. **8**, 43 (1974)].
[11]A. B. Shabat, Dokl. Akad. Nauk SSSR **211**, 1310 (1973).
[12]I. A. Kunin, Teoriya uprugikh sred s mikrostrukturoĭ (Theory of elestic media with micro-structure) Nauka, 1975, Ch. V.
[13]T. A. Gorbushina, L. M. Degtyarev, R. Z. Sagdeev, V. D. Shapiro, and V. I. Shevchenko, Preprint No 17, Inst. Appl. Math. Acad. Sc. USSR, Moscow, 1978.
[14]L. D. Landau and E. M. Lifshitz, Mekhanika sploshnykh sred (Mechanics of Continuous Media) Gostekhizdat, 1954 [English translation published by Pergamon Press, Oxford].

Translated by D. ter Haar

Expansion of collisionless plasma in a vacuum

V. G. Eselevich and V. G. Faĭnshteĭn

Institute of Terrestrial Magnetism and Radiowave Propagation, Siberian Division, USSR Academy of Sciences

(Submitted 1 February 1980)
Zh. Eksp. Teor. Fiz. **79**, 870–882 (September 1980)

The expansion, in a vacuum, of a collisionless plasma with a front of width $\Delta < 10r_D$ and $\Delta \gtrsim 10r_D$ is investigated experimentally. [$r_D=(T_e/4\pi ne^2)^{1/2}$ is the local Debye radius determined by the plasma parameters at the crest of the front; $n\approx 10^7$–10^{10} cm^{-3}, $T_e\approx$ 2–10 eV]. It is shown that as the front moves away from the source, the action of the force of the electronic pressure gradient produces on the front a continuous acceleration of the ions to velocities much higher than the velocity of ion sound. The electronic heat conduction, which supplies energy to the electrons that accelerate the ions, turn out to be much less than in the case of a collisionless plasma. The physical aspect of these processes is investigated in detail.

PACS numbers: 52.30. + r

I. INTRODUCTION

Expansion of a collisionless plasma in a vacuum is one of the important phenomena in plasma physics. Its effects play a substantial role in the acceleration of charged particles in laboratory and cosmic plasma, in the flow of plasma out of stars and in laser-mediated thermonuclear fusion. Many aspects of this phenomena, however, remain unclear to this day.

Ion acceleration in the expansion of the plasma in a vacuum was observed in many experiments, starting with Tanberg's 1930 work[1] (see, e.g., Refs. 2–4). An explanation for this effect, on the basis of the mechanism of ambipolar ion acceleration by electrons, was proposed by Plyutto.[4] A more rigorous treatment of the problem of expansion of a collisionless plasma in a vacuum, assuming a constant electron temperature T_{e0}, was carried out by A.V. Gurevich *et al.*[5] One of

0038-5646/80/090441-08$02.40

the conclusions of their work was that some of the ions can be accelerated by the produced electric field, to velocities u of the order of the electron thermal velocity v_{Te0}. This result was subsequently confirmed by a numerical computer solution of an analogous problem, with allowance for the violation of the quasineutrality on a front of the expanding plasma.[6] In laboratory experiments on the spreading of a plasma in vacuum, the maximum registered velocities of the accelerated ions amounted to several times the speed of ion sound[7-10] ($c_{s0}=\sqrt{T_{e0}/m_i}$), namely $u_{max}\approx(2-3)c_{s0}$, with $E_{max}=m_i u_{max}^2/2\approx(2.0-4.5)T_{e0}$. Since the ion velocity must increase continuously with increasing distance between the front and the source,[6] the results of the experiments should be regarded as too low, since 1) the velocity measured there was *averaged* over the length from the source to the observation point[7,8,10,11]; 2) the maximum distance to the observation point was small and did not exceed 20–40 cm.[7-10] In a number of studies[8,11] the underestimate of u_{max} was due also to the fact that the operating time of the source was comparable with or less than the time of flight of the ion from the source to the observation point. Ion acceleration to velocities $u\gg c_{s0}$ was first observed in Ref. 12. It turned out that as a result of the development of the instability the electron thermal conductivity, which supplies energy to the electrons that accelerate the ions, is much less than it should be in the case of a collisionless plasma.

In the present paper, which is a continuation of Ref. 12, we study the physical laws that govern the expansion of a tenuous plasma in a vacuum. Principal attention is paid to the study of the leading front of the plasma.

II. DIAGNOSTICS APPARATUS AND METHODS

The experiments were performed in a cylindrical vacuum chamber (length 200 cm, diameter 60 cm) evacuated to 5×10^{-6} Torr, in one end of which was located a plasma source 1 (see Fig. 1).[14] The plasma was produced in the source by ionizing pulse-fed gas (argon[1)]) in the gaps (4–15 mm) between the coils 4 and the housing 15, and its parameters were $n_0\approx(10^8-10^{10})$ cm^{-3} and $T_{e0}\approx(2-10)$ eV. The plasma density n_0 at the point of its production (near the coils) increased during the time $t\approx5-10$ μsec after the start of operation of the source, after which it remained constant for several hundred microseconds. The electron temperature T_{e0} hardly changed at $t\gtrsim0.5-1.0$ μsec. The plasma flowed out of the region near the coils as a single stream uniform over the source cross section. The width of the leading front of the flux at the exit from the source 1 ($0x=3$ cm) was 0.5–15 cm, depending on the discharge conditions. The electron and ion mean free paths with respect to collisions with neutral atoms was $\gtrsim10^2$ cm. The distance along the x axis was reckoned from the end of the source. The duration of the source operation, determined by the duration Δt of the voltage pulse accelerating the electrons from the coils to the anode (housing), was in most experiments ~3 msec, i.e., much longer than the time of flight of the plasma over the length of the chamber. The source was also operated at small $\Delta t\approx15-20$ μsec $\ll\tau$.

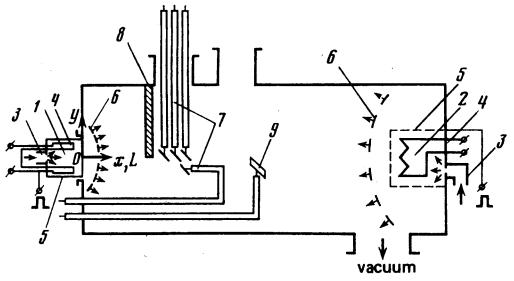

FIG. 1. Diagram of experimental setup: 1 and 2—plasma sources, 3—pulsed valve, 4—incandescent cathode, 5—housing of source 1, 6—plasma front, 7—Langmuir probes, 8—metallic plate covering half the chamber section, 9—multigrid electron analyzer.

The plasma was expanded in the vacuum both as it flowed out of the source along the x axis of the chamber, and as it flowed around a metallic plate 8 under a floating potential, placed at a distance $x=49$ cm and covering half the chamber cross section. In this case we investigated the plasma of flow established behind the plate at ~150–200 μsec after the start of operation of the source, with parameters $n_0\approx10^7-5\times10^8$ cm^{-3}, $T_{e0}\approx4-8$ eV, and $M_s=u_0/c_s\approx2.0-2.5$.

On the second flange of the chamber was located a source 2 similar to that used in Ref. 15. It was used in the experiments on "plasma in plasma" expansion to produce a plasma stream of lower density, $n_1<n_0$, moving towards the source 1 and having near it the parameters $n_1\approx10^6-5\times10^7$ cm^{-3}, $T_{e1}=4-8$ eV, and $T_{e1}/T_{i1}\approx2-4$.

The measurements of the ion density, the electron temperature, the plasma potential, as well as the velocity of the plasma front were made by a cylindrical Langmuir probe 7 (length 10 cm, diameter 0.05 cm), movable along the chamber axis.[16] In individual control experiments, when sufficiently narrow fronts with $\Delta\lesssim1-2$ cm were registered, the spatial resolution was improved by using, as a flat probe with entrance aperture 20–30 mm, a multigrid analyzer with registration based on a microchannel plate (MCP). This analyzer was used to measure the ion energy on the front of the expanding plasma.[17]

The plasma motion along the y axis in the case of flow around a plate was investigated by three cylindrical Langmuir probes 7, movable along the radius of the chamber. The positions of these probes relative to the plate were respectively $x_{01}=1,0-1.5$ cm, $x_{02}=3-4$ cm, $x_{03}=5.5-7.5$ cm. The time resolution of the probes τ_r (without allowance for the plasma–probe transition layer) were determined by the load resistance and by the parasitic capacitance of the conducting cable and varied in different experiments from 1.5 μsec to 10^{-2} μsec. Measurement of the electron temperature in the front and in the rear regions of the plasma stream were made with an electron multigrid analyzer 9 with energy resolution $\lesssim0.5$ eV.

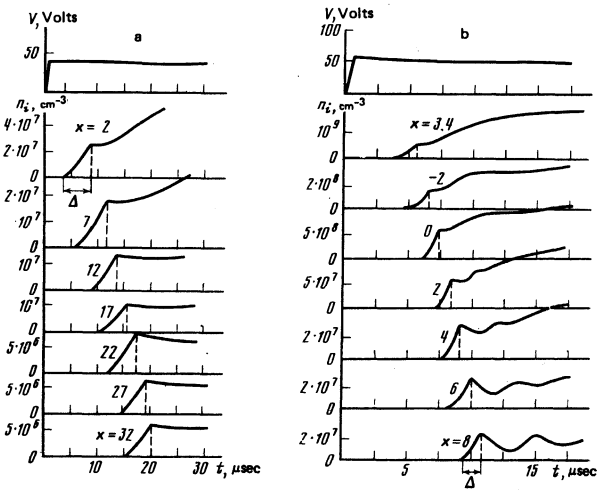

FIG. 2. Time dependences of the ion density of a plasma expanding in a vacuum at various distances x from the source: a—$\Delta \gtrsim 10r_D$, b—$\Delta < 10r_D$ (top-voltage on the source at $\Delta t \approx 3$ μsec).

III. EXPERIMENTAL RESULTS

The time dependences of the ion density $n_i \approx n$ of the plasma escaping from the source 1 into the vacuum, at different distances x, for cases when the front width is $\Delta > 10r_D$ and $\Delta < 10r_D$, are shown in Fig. 2a and 2b respectively [$r_D = (T_e/4\pi ne^2)^{1/2}$ is the local Debye radius determined by the values of n and T_e at the crest of the front]. Sequences of such oscillograms make it possible to determine the front velocity u as a function of x (Fig. 3b) and the front width[2] $\Delta(n)$ (Fig. 4), and to plot the spatial distributions of n in various successive instants of time (Fig. 5).

As the plasma moves away from the source, the density n at the crest of the front decreases noticeably (see Fig. 5) [T_e changes relatively little in this case (Fig. 3a)]. Consequently r_D increases and, accordingly, the ratio Δ/r_D decreases. At sufficiently large values of n, such that $\Delta/r_D > 10$, Δ is practically independent of n, i.e., the plasma expands in the vacuum along x at a constant (within ±15%) front width Δ (Figs. 5a and 4a). In Fig. 5b, the condition $\Delta/r_D > 10$ is satisfied only near the point where the plasma is produced ($x < -2$ cm). At a distance $x > -2$ cm, Δ becomes less than $10r_D$ and varies approximately like $1/n^{1/2}$ with further motion [Fig. 5b (curves 2,3), Fig. 4b[3]]. This

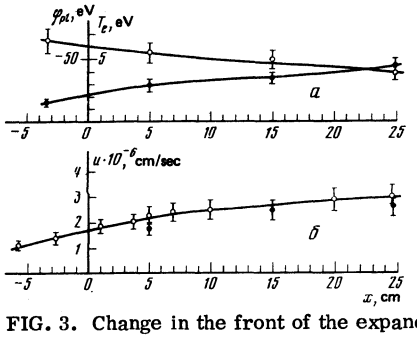

FIG. 3. Change in the front of the expanding plasma with changing distance x: a—of the electron temperature T_e(○) and of the plasma potential φ_{pl}(●); b—of the ion velocity u.

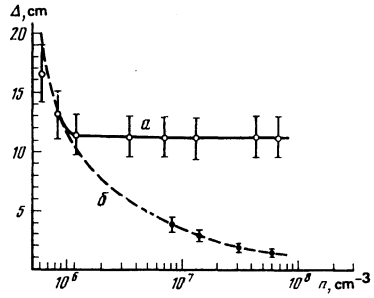

FIG. 4. Dependence of the width Δ of the plasma front on the local density n: a—$\Delta \gtrsim 10r_D$, b—$\Delta < 10r_D$ the dashed curve corresponds to $\sim n^{-1/2}$.

is accompanied by a phenomenon similar to dispersion, namely the appearance of density oscillations lagging the front, with characteristic wavelength $\sim\lambda_D \approx 2\pi r_D$. In the course of motion, the ion velocity on the front increases continuously with increasing x (Fig. 3b). (The values of u on Fig. 3b, marked by black circles, are obtained by measuring the energy of the ions with the multigrid analyzer with a registration system using a microchannel plate.) As shown earlier,[12] an increase in velocity was observed up to the maximum value $x_{max} = 150$ cm at which registration of the channel n_i was still possible. The velocities of the ions accelerated on $x_{max} = 150$ cm were $u \gtrsim 15c_{s0}$, corresponding to $E \gtrsim 100T_{e0}$. As seen from Fig. 6, the electron distribution function $f_e(E_e)$ was nearly Maxwellian in this case not only in the principal region of the velocities, but also at $E_e \gtrsim 10T_e$ (E_e is the electron energy). Measurement of $f_e(E)$ at $E \gg 10T_e$ was limited by the sensitivity of the multigrid electron analyzer.[17]

Acceleration of the ions by electrons along x is accompanied by an increase in the negative plasma potential φ_{pl} (Fig. 3a). If the electrons have a nearly Boltzmann distribution, $n \sim n_0 \exp(e\varphi_{pl}/T_e)$ then φ_{pl} is connected with the change of n along x (at $T_e \approx$ const) by the relation[5]

$$\varphi_{pl} \approx -T_e \ln (n_0/n). \qquad (1)$$

Estimating for the instant of time $t \approx 10$ μsec (Fig. 5b) the change of the potential between the points $x = -2$ cm ($n \approx 2 \cdot 10^8$ cm^{-3}) and $x = 8$ cm ($n \approx 1.3 \cdot 10^7$ cm^{-3}) at $T_e \approx 6$ eV, we find that $\Delta\varphi_{pl} \approx -16$ eV, in satisfactory

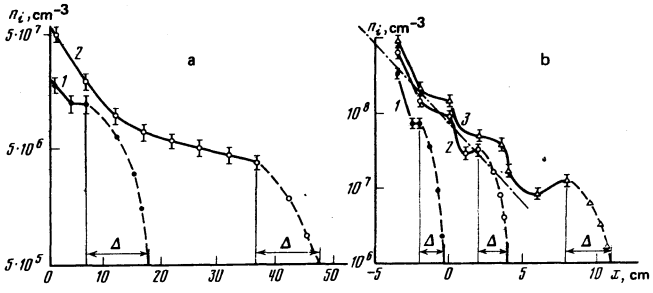

FIG. 5. Spatial distributions of the ion density n_i of a plasma expanding in a vacuum with a front of width $\Delta \gtrsim 10r_D$ (a) and $\Delta < 10r_D$ (b) at various instants of time: a—$t \approx 12$ μsec (1), $t \approx 21$ μsec (2); b—$t \approx 5.6$ μsec (1), $t \approx 7.6$ μsec (2), $t \approx 10$ μsec (3).

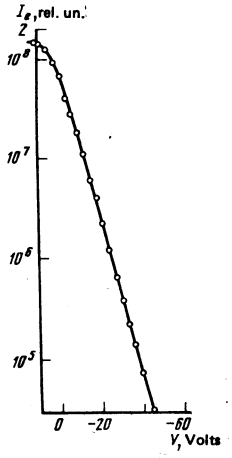

FIG. 6. Dependence of the electron current in a multigrid electron analyzer on the voltage on the "decelerating" grid. $x = 10$ cm, $n \approx 4 \times 10^8$ cm^{-3}, and $T_e \approx 6$ eV.

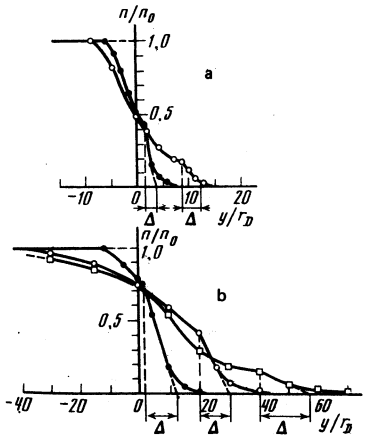

FIG. 7. Initial stage of expansion of a plasma in vacuum in flow around a plate. Dependence of the ion density n_i on the distance y for different positions x_{0j} relative to the plate and for different n_0 at $T_{e0} \approx 4$ eV: a—$n_0 \approx 2 \times 10^7$ cm^{-3}, $x_{01} = 1.5$ cm (●), $x_{02} = 5.5$ cm (○); b—$n_0 \approx 4 \times 10^8$ cm^{-3}, $x_{01} = 1.5$ cm (●), $x_{02} = 4$ cm (○), $x_{03} = 7.5$ cm (□).

agreement with the measured $\Delta\varphi_{p1} \approx -13$ eV (Fig. 3a).

Under the stationary boundary conditions $n_0(t) \approx$ const (in our case this is valid at $t \gtrsim 10$ μsec) the expected dependence of the density n on the time t is[18]

$$n \sim t^{-2}. \tag{2}$$

Under experimental conditions, a relation close to (2) is satisfied at $t > 10$ μsec for the front, where the quasineutrality is violated ($\Delta < 10r_D$) (see Fig. 1 of Ref. 12), for a quasineutral front ($\Delta \gtrsim 10r_D$, Fig. 5a), and for other sections of the distribution $n(x)$ (e.g., $x = 0$–5 cm, Fig. 5a). At $t < 10$ μsec [$n_0(t) \neq$ const] the $n(t)$ dependence differs from (2) (Fig. 5b).

The construction of source 1 (Fig. 1) did not permit measurements to be made closer than ≈5 cm from the point of plasma production. Therefore the initial stage of the plasma expansion ($x < -4$ cm) was investigated with the plasma flowing around a metallic plate 8 (Fig. 1). The experimental geometry was nearly planar, and the boundary conditions were quasistationary [$n_0(t) \approx$ const during the time of observation].

The spatial distributions of the ion density at various distances x_{0j} from the plate (behind the plate) for $\Delta < 10r_D$ are shown in Fig. 7 [here Δ is the width of the plasma front moving along y (along the radius)]. Inasmuch as the plasma-flow parameters along the axis of the chamber, remain practically unchanged on the segment of length x_{03} between the plate and the far probe, the pictures of the distributions n with respect to y in different sections along x are equivalent to the n profiles of a plasma moving along y at successive instants of time: $t_{0j} = x_{0j}/u_0$ the velocity of the front along y, measured between the i-th and the j-th probes, is connected with u_0 by the relation $u_{ij} \approx u_0 y_{ij}/x_{ij}$, where y_{ij} is the displacement of the front along y when the flow negotiates along x the distance x_{ij} between probes i and j.

In both cases, $\Delta < 10r_D$ and $\Delta \gtrsim 10r_D$, during the initial stage of expansion along y ($x_{01} \approx 1$ cm), the widths of the fronts are $\Delta \sim (2T_{i0}/m_i)^{1/2} x_{01}/u_{01} \approx 1$ cm (Fig. 7), i.e., they are determined by the thermal scatter of the plasma ions prior to the start of its expansion in the vacuum. With further motion of the front along y, just as in the previously considered case of a plasma escaping into vacuum from the source 1, the width of the front either does not change with distance if $\Delta \gtrsim 10r_D$ (Fig. 4a), or increases approximately like $n^{-1/2}$ if $\Delta < 10r_D$ (Fig. 4b).

According to Ref. 6, in the case of cold ions and constant T_e, it follows from the Poisson equation and from the requirement that the potential φ_{p1} and its derivative $d\varphi_{p1}/dy$ be continuous in the front at all y, that

$$\frac{1}{8\pi}\left(\frac{d\varphi_{p1}}{dy}\right)^2 = n_e T_{e0}. \tag{3}$$

The width of the front at the initial instant at $t = 0$ and $y = 0$ is obtained by substituting in (1) the values $\varphi_{p1} = -T_{e0}/e$ and $n_e = n_0 e^{-1}$.[6] From this we get

$$\Delta \approx r_D. \tag{4}$$

Since T_e is constant when the front moves, it follows that $\Delta \sim n^{-1/2}$. Under the experimental conditions, since $T_{i0} \neq 0$, the width of the front Δ at $y = 0$ is determined by the thermal scatter of the ions. However, with acceleration of the front of the plasma that moves into the vacuum, the longitudinal (along u) effective ion temperature in the fronts should decrease rapidly.[5] This explains apparently why the fronts with $\Delta \gtrsim 10r_D$ propagate in the vacuum with almost constant Δ, while the fronts with $\Delta \sim r_D < 10r_D$ vary with distance like $n^{-1/2}$, owing to the violation of the quasineutrality in the front.

We now compare the experimental results of the study of the flow of the plasma out of source 1 and around the plate, with the results of calculations[6] of the dynamics of expansion, in vacuum, of a plane boundary of a collisionless plasma with $T_{i0} = 0$ at constant T_e. To this end we consider the dependence of $M_s = u(T_{e0}/m_i)^{-1/2}$ on $\omega_{0i}t$. Here $\omega_{0i} = (4\pi n_0 e^2/m_i)^{1/2}$, t is the time in which the plasma front covers the distance $y(x)$ from the start of the motion $y = 0, x = 0$.

Curves b and c on Fig. 8 correspond to fronts with $\Delta < 10r_D$ and $\Delta \gtrsim 10r_D$, observed in flow around a plate

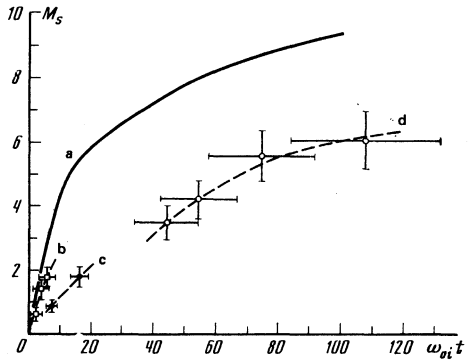

FIG. 8. Dependence of the velocity of the plasma front moving in vacuum on the time: a—calculation,[6] b—$r_D \lesssim \Delta < 10r_D$, c, d—$\Delta \gtrsim 10r_D$.

(see Fig. 6), curve d corresponds to the front of a plasma with $\Delta > 10r_D$, flowing along x from the source 1, and a is the calculated curve.[6] To plot curve d we used the data of Figs. 2b and 5b. The density n_0 at different instants of time at the point of plasma production near the coils (equivalent to $x \approx -8$ cm) was obtained by extrapolating the straight dash-dot curve of Fig. 5b, with allowance for the change of density with time which takes place at $t < 10$ μsec.

It follows from Fig. 8 that the fastest growth of M_s with time (distance) corresponds to the calculated curve with $T_{i0} = 0$. Allowance for T_{i0} leads to a decrease of M_s.[19] This is apparently one of the reasons why the experimental curve b for $\Delta \approx r_D$ lies lower than the curve a. The larger the width Δ of the front, the slower the increase of its velocity with time (distance) (curves c and d lie lower than b on Fig. 8). The reason for this can be understood from the following estimate. At $T_{i0} \ll T_{e0}$ and $T_e \approx$ const the force accelerating the ions in a plane plasma front moving in vacuum is the gradient of the electron pressure. Then the acceleration a is given by

$$a = \frac{d^2y}{dt^2} \simeq -\frac{z}{m_i}\frac{1}{n}\frac{d(nT_{e0})}{dy} \approx \frac{zT_{e0}}{m_i}\frac{1}{\Delta(y)}, \tag{5}$$

$z = 1$ is the charge of the ion in our case.

Integrating (5) we obtain

$$u^2(y_2) \approx u^2(y_1) + \frac{2T_{e0}}{m_i}\int_{y_1}^{y_2}\frac{dy}{\Delta(y)}. \tag{6}$$

Estimates of u and a by formulas (5) and (6) agree in order of magnitude with the experimental values. It follows from (5) that the observed decrease of the acceleration with increasing x (the slope of the curve of Fig. 3b) is connected principally with the increase of $\Delta(x)$. Under the conditions of our experiment, during the initial stage of the expansion of the plasma into vacuum, near $y = 0$ the velocity $u(0) \sim (2T_{i0}/m_i)^{1/2} = v_{T_{i0}}$. Since $T_{i0} \lesssim 1$–2 eV, we have already at distances corresponding to $\omega_{0i}t \gtrsim 50$, a value $u \gg v_{T_{i0}}$ (Fig. 8d) and expression (6) takes the simpler form

$$u(y) \approx \left(\frac{2T_{e0}}{m_i}\int_0^y \frac{dy}{\Delta(y)}\right)^{1/2}. \tag{7}$$

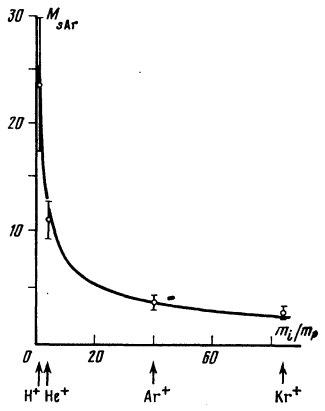

FIG. 9. The dependence of the plasma-front velocity, normalized to the velocity of the ion sound in argon $c_{sAr} = (T_{e0}/m_{iAr})^{1/2}$, on the ion mass normalized to the hydrogen m_p, at the exit from the source ($x \approx 3$ cm, $T_{e0} \approx 4$ eV, $\Delta \approx 6$–8 cm).

The function $u \sim (T_{e0}/m_i)^{1/2}$ is obtained also from calculations,[6] inasmuch as the quantity plotted in Fig. 8a is the velocity u normalized to $(T_{e0}/m_i)^{1/2}$.

Figures 9 and 10 show respectively experimental plots of the normalized velocity $M_{sAr} = u(T_{e0}/m_{iAr})^{-1/2}$ against the ion mass m_i/m_p (we used H^+, He^+, Ar^+, Kr^+) and of the velocity u against T_{e0} for Ar^+, measured at a distance equivalent to $\omega_{0i}t \approx 50$–80. The curves in Fig. 9 and 10 are respectively plots of $\sim 1/m_i^{1/2}$ and $\sim (T_{e0})^{1/2}$.

The foregoing outlines the following qualitative picture of the expansion of a collisionless non-isothermal ($T_{e0} > T_{i0}$) plasma in a vacuum.

The start of the motion of the plasma boundary into the vacuum takes place at a velocity $\sim v_{T_{i0}}$. Since the thermal velocity of the electrons $v_{T_{e0}} \gg v_{T_{i0}}$, the electrons, leading the ions by $\sim r_D$, drag the ions behind them by means of the action of the electric field. The force that causes the acceleration of the ions in the front is the electron-pressure gradient. Giving up thermal energy to the ions in this process, the electrons should cool down. Therefore continuous acceleration of the ions along the entire path x from the source is possible only in the presence of a constant influx of electronic heat from the source to the front. This means primarily that the duration Δt of the operation of the source should be longer than the time τ of travel of the plasma over the observed length. In the experiments described above this condition was satisfied.

Figure 11 shows the dependence of u on x for the case

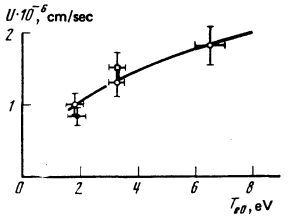

FIG. 10. Dependence of the velocity of the plasma front at the exit from the source ($x \approx 3$ cm) on the electron temperature T_{e0}: □—$\Delta \approx$ (3–4) cm, ○—$\Delta \approx$ (6–7) cm, ●—$\Delta \approx 10$ cm.

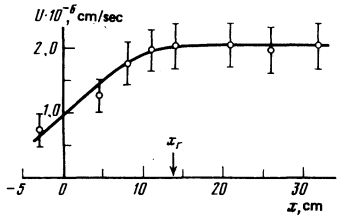

FIG. 11. Dependence of the plasma-front velocity on the distance x at the short time of source operation $\Delta t \approx 15$–20 μsec.

of a short duration of the source operation $\Delta t \approx (15–20)$ μsec. It is seen that the acceleration of the ions as they move takes place in a time $\sim x_g/u_{av} \approx 20$ μsec, i.e., it is comparable with the operating time of the source. At $x > x_g$ the expansion of the plasma with the source turned off takes place at practically constant velocity.

Measurements of the electron temperature in the front and during the following instants of time behind the front at various distances from the source have shown that T_e decreases with increasing x at $\Delta t \gg \tau$, and this decrease exceeds by more than one order of magnitude the decrease of T_e due to the cooling of the electrons as a result of collisions with a moving front.[13] This means that the electronic thermal conductivity, which ensures the electronic heat flow q from the source to the front, is substantially higher than it should be in the case of a collisionless plasma.

To determine the reason for this, measurements were made of the ion density of the expanding plasma at various distances x with a Langmuir probe and with an improved time resolution $\tau_r \approx 0.01$ μsec [in all the preceding measurements, $\tau_r \approx R_L C_c \approx (0.5–2.0)$ μsec, where R_L is the load resistance and C_c is the capacitance of the supply cable]. These measurements have shown that with increasing distance from the source in the region of the front and behind the front, the level of electrostatic oscillations of the density increases.

The oscillations of the electron current I_b were observed with a cylindrical Langmuir probe using the circuits shown in Fig. 12. The probe voltage $V_p = +9$ V exceeded the plasma potential φ_{pl} by $(0–3)T_e$. All the measurements were made at an instant $t = 100$ μsec after the start of the source operation. The high-frequency (HF) oscillations ($\omega_{0i}/2\pi \ll f \lesssim \omega_{0e}/2\pi$) were registered in the frequency band 5×10^6 Hz $\lesssim f \lesssim 6 \times 10^7$ Hz, and the low-frequency (LF) oscillations $f \lesssim \omega_{0i}/2\pi$ in the band 10^5 Hz $\lesssim f \lesssim 5 \times 10^6$ Hz.

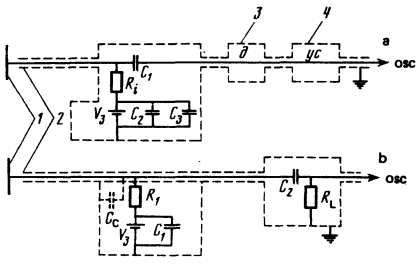

FIG. 12. Measurement circuits: a—high frequency oscillations (5×10^6 Hz $\lesssim f \lesssim 6\times10^7$ Hz): 1—Langmuir probe, 2—cable, 3—matched divider, 4—amplifier; b—low-frequency oscillations (10^5 Hz $\lesssim f \lesssim 5\times10^6$ Hz): $R_1 \approx$ (75–300) Ω, $R_L \approx$ (18–24) $k\Omega$, $C_c \approx$ (200–300) pF, $C_1 = 2.0$ μF, $C_2 = (270–300)$ pF, $V_{pr} = +9$ V, $R_i = 75$ Ω.

The time dependences of the HF and LF oscillations I_e in the corresponding amplitude-frequency spectra $G(f)$ were obtained by computer reduction of the oscillograms using the formula[20]

$$G(f) \approx 2 \int_0^\infty \left[\int_0^T I_e(t) I_e(t+\tau)\, dt \right] e^{-2\pi i f \tau}\, d\tau. \qquad (8)$$

The complete spectrum (with allowance for the LF and HF oscillations) constitutes two maxima greatly separated in frequency, one near $f_1 \sim (\frac{1}{3}-1)\omega_{0e}/2\pi$ ($\omega_{0e} = \sqrt{4\pi ne^2/m_e}$) and the other at $f_2 \sim (1–3)(\omega_{0i} + ku)/2\pi$, where $(\omega_{0i} + ku)$ is the frequency of the ion Langmuir oscillations with allowance for their dragging by the plasma flow.

The wavelength of the oscillations with the largest amplitude was estimated from simultaneous measurements by two probes with variable distance between them. It is seen from Fig. 13 that at $x = 040$ cm a change of phase by π takes place when the distance between the probes becomes 3–4 cm, corresponding to $\lambda \approx 6$–8 cm $\sim 2\pi r_D$ (Figs. 13a_1 and 13a_2). At $x = 15$ cm the wavelength is $\lambda \approx 2$–3 cm $\sim 2\pi r_D$ (Figs. 13b_1 and 13b_2). It follows therefore that the plasma oscillations (electron and ion Langmuir oscillations) are primarily excited, and the ion-sound oscillations have the smaller amplitudes.

We note that the amplitude-frequency spectrum measured with the Langmuir probe reflects correctly the true spectrum of oscillations only at 1) $10^5 \lesssim f \lesssim \omega_{0i}/2\pi$ and 2) $\omega_{0i}/2\pi \ll f \lesssim \omega_{0e}/2\pi$. The reason is that in the first case the time resolution of the layer next to the sound, determined by the inertia of the ions, is $\tau_{pr} \sim 1/\omega_{0i}$ while in the second τ_{pr} is determined by the inertia of the electrons and amounts to $\sim 1/\omega_{0e}$. At $\omega_{0i}/2\pi < f \ll \omega_{0e}/2\pi$, the inertia of the ions should distort the true spectrum of the oscillations.

The possible causes of the buildup of oscillations can be the following.

1. The deviation of the distribution function of the electron velocity from Maxwellian.[21]

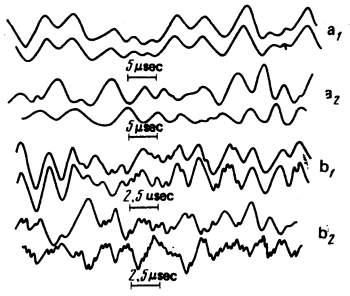

FIG. 13. Time dependences of the low-frequency oscillations, obtained simultaneously by Langmuir probes located at different distances x_1 and x_2 from the source: a_1) $x_1 = x_2 = 45$ cm, a_2) $x_1 = 45$ cm, $x_2 = 42$ cm; b_1) $x_1 = x_2 = 15$ cm, b_2) $x_1 = 15$ cm,, $x_2 = 16$ cm the distance along y between probes is 0.5 cm.

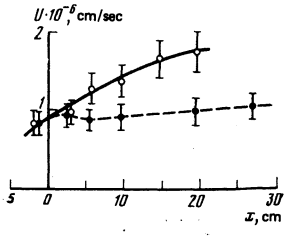

FIG. 14. Comparison of the dependences of the plasma front velocity u on the distance x in the case of expansion: a—in a vacuum, b—in a plasma ($T_{e0} \approx 7$ eV).

2. The presence of electron beams from the source.

3. The disequilibrium of the electron energy distribution function $f_e(E)$ as a result of the weak electron-temperature gradient along x, which appears because of the finite rate of transport of the electronic heat along x. In the quasicollision case, this instability was considered theoretically in Refs. 22 and 23.

As seen from Fig. 6, the distribution function is close to Maxwellian at a probe electron current that changes by almost four orders of magnitude. This makes it possible to exclude to some degree the causes 1 and 2, and to regard as the most probable cause of the buildup of instability to be the third, connected with the disequilibrium of $f_e(E_e)$.[4)] The presence of random oscillations, which is equivalent to effective collisions, is the probable cause of the decrease of the electronic thermal conductivity (and correspondingly of the decrease of T_e as a function of x), observed in the experiments.

When a collisionless plasma of density n at the crest of the front was expanded in a plasma of lower density $n_1 < n$ produced by source 2 (Fig. 1), we observed a collective interaction of the two plasmas, manifesting itself in the following:

a) An increase of the level of electrostatic oscillations of the density n_i in the front and behind the front, with characteristic frequency $\lesssim \omega_{0i}/2\pi$, and a simultaneous transformation of the front.

b) Deceleration of the front compared with its velocity into vacuum, Fig. 14.

The distance x at which the collisionless slowing down of the front comes into play was determined by the relation $n_1 \gtrsim n/10$. The most probable cause of these effects, taking the character of the observed random oscillations into account, can be assumed to be the buildup of ion-ion instability due to the relative motion of the plasma streams, analogous to that observed in Ref. 24.

CONCLUSIONS

1. Expansion of a collisionless plasma in vacuum takes place with a front whose width Δ, depending on the local parameters (T_e, T_i, n), can be $r_D \lesssim \Delta < 10 r_D$ or $\Delta \gtrsim 10 r_D$. At $\Delta \gtrsim 10 r_D$ the width of the front hardly varies with distance, within the limits of experimental error. At $\Delta < 10 r_D$, owing to violation of the quasineutrality, Δ varies with distance approximately like $n^{-1/2}$.

2. The force that accelerates the ions on the plasma front in the course of expansion in vacuum is the gradient of the electron pressure. Consequently, the plasma velocity as it emerges from the source increases in proportion to $(T_{e0}/m_i)^{1/2}$ and decreases with increasing Δ. At $\Delta \gtrsim r_D$, the initial expansion stage agrees satisfactorily with a calculation[6] performed for the planar case at $T_e = \text{const}$.

3. The increase of the front velocity with the source in operation takes place continuously on the entire path of the source motion. At large distances from the source ($x = 150$ cm) the value of u can reach $\gtrsim 15 c_{s0}$, corresponding to an energy $E \gtrsim 100\, T_{e0}$. After the source is turned off, the plasma front continues to move at constant velocity.

4. The electronic heat conduction, which supplies energy to the electrons that accelerate the ions, is much smaller, owing to the development of instability, than it should be in the case of a collisionless plasma,

5. When a plasma front with density n expands in a background plasma with density $n_1 < n$, a collisionless deceleration of the front is observed and is apparently connected with development of ion-stability.

The authors are grateful to D.D. Ryutov, A.V. Gurevish, B.N. Breĭzman, and E.V. Mishin for a discussion of the results, and to N.V. Astrakhantsev for help with the reduction of the oscillograms of the oscillations.

[1)] In the investigation of the dependence of u on the ion mass we used hydrogen, helium, argon, and krypton.
[2)] Δ was defined as double the width of the front at its half-height (see Fig. 2).
[3)] The cylindrical Langmuir probe used to measure n_i yields $\Delta_{min} \approx (6-7) r_D$. The flat Langmuir probe used for the ion current registered $\Delta_{min} \approx (3-6) r_D$.
[4)] In certain operating regimes of the source, $f_e(E)$ has a doubly Maxwellian form. In these cases, the first cause can play a definite role in the buildup of the oscillations.

[1] R. Tanberg, Phys. Rev. 35, 1080 (1930).
[2] E. Kobel, Phys. Rev. 36, 1636 (1930).
[3] L. Tonkes, Phys. Rev. 54, 634 (1938).
[4] A. A. Plyutto, Zh. Eksp. Teor. Fiz. 39, 1589 (1960) [Sov. Phys. JETP 12, 1106 (1961)].
[5] A. V. Gurevich, L. V. Pariĭskaya, and L. V. Pitaevskiĭ, *ibid.* 49, 647 (1965) [22, 449 (1966)].
[6] J. E. Crow, P. L. Awer, and J. E. Allen, J. Plasma Physics 14, 65 (1975).
[7] P. F. Little, Journal of Nuclear Energy, part C, 4, 15 (1962).
[8] H. W. Hendel and T. T. Reboul, Phys. Fluids 5, 360 (1962).
[9] A. A. Plyutto, V. N. Ryzhkov, and A. T. Kapin, Zh. Eksp. Teor. Fiz. 47, 494 (1964) [Sov. Phys. JETP 20, 328 (1965)].
[10] M. A. Tyulina, Zh. Tekh. Fiz. 35, 511 (1965) [Sov. Phys. Tech. Phys. 10, 396 (1965)].
[11] G. C. Goldenbauk and K. A. Gerber, Phys. Fluids 16, 1289 (1972).
[12] V. G. Eselevich and V. G. Faĭnshteĭn, Dokl. Akad. Nauk SSSR 244, 1111 (1979) [Sov. Phys. Doklady 24, 114 (1979)].
[13] J. Denavit, Phys. Fluids 22, 1384 (1979).
[14] V. G. Eselevich, Yu. S. Karavaev, V. I. Koroteev, and V. G. Faĭnshteĭn, SibIZMIR (Siberian Inst. Terr. Magn. and Radiowave Propagation) Preprint No. 18, 1977.

[15]O. L. Volkov, V. G. Eselevich, G. N. Kichigin, and V. L. Papernyĭ, Zh. Eksp. Teor. Fiz. 67, 1689 (1974) [Sov. Phys. JETP 40, 841 (1975)].
[16]N. V. Astrakhantsev, O. L. Volkov, V. G. Eselevich, G. N. Kichigin, and V. L. Papernyĭ, *ibid.* 76, 1289 (1979) [48, 649 (1979)].
[17]V. G. Eselevich and V. G. Faĭnshteĭn, SibIZMIR Preprint No. 15, 1980.
[18]K. E. Lonngren and N. Hershkovich, IEEE Trans., Plasma Sciences PS-7, 107 (1979).
[19]S. I. Anisimov and Yu. V. Medvedev, Zh. Eksp. Teor. Fiz. 76, 121 (1979) [Sov. Phys. JETP 49, 62 (1979)].
[20]J. S. Bendat and A. G. Piersol, Random Data: Analysis and Measurement Procedures, Wiley, 1968 (Russ. transl. Mir, 1974, p. 38).
[21]A. Gurevich, D. Anderson, and H. Wilhelmson, Phys. Rev. Lett. 42, 769 (1979).
[22]D. W. Forslund, J. Geophys. Res. Space Phys. 75, 17 (1970).
[23]E. V. Mishin, Dokl. Akad. Nauk SSSR 215, 565 (1974) [Sov. Phys. Doklady 19, 140 (1974)].
[24]V. G. Eselevich and V. G. Faĭnshteĭn, SibIZMIR Preprint No. 35, 1978.

Translated by J. G. Adashko

Coherent Mössbauer scattering in birefringent crystals

E. V. Smirnov and V. A. Belyakov

All-Union Research Institute for Physicotechnical and Radiotechnical Measurements
(Submitted 18 July 1979)
Zh. Eksp. Teor. Fiz. 79, 883–892 (September 1980)

Coherent scattering of Mössbauer γ radiation in magnetically ordered birefringent crystals is theoretically considered. It is shown that Mössbauer scattering by such crystals has a number of features that distinguish it from the case when there is no birefringence of the γ quanta in the crystal. Analytic expressions that describe the intensity and the polarization characteristics of the scattering are obtained for the case of strong birefringence, and their connection with the details of the magnetic structure of the crystal and with the magnitude of the birefringence is analyzed. It is shown that in this case the coefficient of reflection of the γ quanta from the crystal, as a function of the incidence angle, of the orientation of the magnetic fields at the nuclei, and of the energy of the γ quanta assumes in this case a complicated (multihump) form. The possibility of experimentally investigating these effects in α-Fe_2O_3 and $FeBO_3$ crystals are discussed.

PACS numbers: 76.80. + y, 78.20.Fm

INTRODUCTION

The study of the diffraction of resonant γ radiation by crystals is now branching out into an autonomous research trend, and progresses vigorously both theoretically and experimentally.[1] A number of interesting properties of Mössbauer diffraction is observed under conditions of hyperfine splitting of a Mössbauer line in a crystal.[2-9] In particular, theoretical investigations of the diffraction of Mössbauer γ quanta by perfect magnetically ordered crystals have revealed peculiarities in Mössbauer dynamic scattering, viz., complicated polarization properties of the scattered radiation[10] and magnetic Pendollosung beats.[11]

This paper deals with Mössbauer scattering of γ radiation by magnetically ordered crystals having strong birefringence. It is shown that the intensity and polarization of the diffracted radiation has a complicated dependence on the energy of the γ quanta, on the orientation of the magnetic fields at the nuclei, and on the angle of incidence of the radiation on the crystal. This dependence is connected with the birefringence of the γ quanta in the crystal and is due to the possibility of varying the birefringence by changing the beam energy or the orientations of the magnetic fields.

The scattering of Mössbauer radiation is considered in detail in the case of thin (kinematic limit) and thick (dynamic theory) perfect crystals, and a detailed analysis is presented of situations that are of interest from the experimental point of view and lend themselves to an analytic description.

SYSTEM OF BASIC EQUATIONS

We consider the scattering of resonant γ radiation by a crystal in the form of a plane-parallel plate, containing Mössbauer nuclei, with the Bragg condition satisfied or nearly so. The γ-radiation field in the crystal is obtained by solving Maxwell's equations, which in the two-wave approximation can be represented in the form

$$\begin{aligned}\gamma_1\frac{d\mathbf{E}_1}{dz}&=\frac{i\varkappa}{2}\hat{F}_{11}\mathbf{E}_1+\frac{i\varkappa}{2}\hat{F}_{12}\mathbf{E}_2,\\ \gamma_2\frac{d\mathbf{E}_2}{dz}&=\frac{i\varkappa}{2}\hat{F}_{21}\mathbf{E}_1+\frac{i\varkappa}{2}(\hat{F}_{22}-\alpha\hat{I})\mathbf{E}_2,\end{aligned}\qquad(1)$$

where $\mathbf{E}_1, \mathbf{E}_2, \gamma_1, \gamma_2$ are the amplitudes and direction cosines of the incident and diffracted waves relative to the normal to the surface, $\varkappa$ is the wave vector of the radiation in vacuum, z is the coordinate along the normal to the sample surface, $\hat{I}$ is a unit matrix of second order, F_{ip} is an operator that describes the scattering, by the unit cell of the crystal, of a wave with wave vector $\mathbf{k}_p$ into a wave with wave vector $\mathbf{k}_i$. The elements of this operator are the scattering amplitudes $F_{ip}^{s's}$, where the superscripts $s, s' = 1, 2$ designate the polarizations of the waves in the primary and secondary directions; the explicit forms of the operators are given in Ref. 10. The wave vectors $\mathbf{k}_1^{(s)}$ and

 0038-5646/80/090448-06$02.40